TECHNICAL REPORT RD-RE-89-2

COMPUTER GENERATED MATCHED FILTERS WITH SPATIAL FREQUENCY TAILORING

Don A. Gregory
Kevin Worchester
Research Directorate
Research, Development, and Engineering Center

Larry Z. Kennedy
Applied Research, Inc.
Huntsville, AL

J. Graeme Duthie
Physics Department
University of Alabama
Huntsville, AL

April 1989

U.S. ARMY MISSILE COMMAND
Redstone Arsenal, Alabama 35898-5000

Approved for public release; distribution is unlimited.

DISPOSITION INSTRUCTIONS

DESTROY THIS REPORT WHEN IT IS NO LONGER NEEDED. DO NOT RETURN IT TO THE ORIGINATOR.

DISCLAIMER

THE FINDINGS IN THIS REPORT ARE NOT TO BE CONSTRUED AS AN OFFICIAL DEPARTMENT OF THE ARMY POSITION UNLESS SO DESIGNATED BY OTHER AUTHORIZED DOCUMENTS.

TRADE NAMES

USE OF TRADE NAMES OR MANUFACTURERS IN THIS REPORT DOES NOT CONSTITUTE AN OFFICIAL INDORSEMENT OR APPROVAL OF THE USE OF SUCH COMMERCIAL HARDWARE OR SOFTWARE.

REPORT DOCUMENTATION PAGE

Form Approved
OMB No 0704-0188
Exp Date Jun 30, 1986

1a. REPORT SECURITY CLASSIFICATION UNCLASSIFIED	1b. RESTRICTIVE MARKINGS
2a. SECURITY CLASSIFICATION AUTHORITY	3. DISTRIBUTION/AVAILABILITY OF REPORT Approved for public release; distribution is unlimited
2b. DECLASSIFICATION/DOWNGRADING SCHEDULE	
4. PERFORMING ORGANIZATION REPORT NUMBER(S) RD-RE-89-2	5. MONITORING ORGANIZATION REPORT NUMBER(S)
6a. NAME OF PERFORMING ORGANIZATION Research Directorate RD&E Center 6b. OFFICE SYMBOL (If applicable) AMSMI-RD-RE	7a. NAME OF MONITORING ORGANIZATION
6c. ADDRESS (City, State, and ZIP Code) Commander U.S. Army Missile Command ATTN: AMSMI-RD-RE Redstone Arsenal, AL 35898-5248	7b. ADDRESS (City, State, and ZIP Code)
8a. NAME OF FUNDING/SPONSORING ORGANIZATION 8b. OFFICE SYMBOL (If applicable)	9. PROCUREMENT INSTRUMENT IDENTIFICATION NUMBER
8c. ADDRESS (City, State, and ZIP Code)	10. SOURCE OF FUNDING NUMBERS PROGRAM ELEMENT NO. / PROJECT NO. / TASK NO. / WORK UNIT ACCESSION NO

11. TITLE (Include Security Classification)

Computer Generated Matched Filter With Spatial Frequency Tailoring

12. PERSONAL AUTHOR(S)
Don A. Gregory

13a. TYPE OF REPORT	13b. TIME COVERED	14. DATE OF REPORT (Year, Month, Day)	15. PAGE COUNT
Final	FROM Jun 88 TO Oct 88	April 1989	43

16. SUPPLEMENTARY NOTATION

17. COSATI CODES			18. SUBJECT TERMS (Continue on reverse if necessary and identify by block number)	
FIELD	GROUP	SUB-GROUP	Optical Computing	Matched Filtering
			Computer Generated Holography	Pattern Recognition

19. ABSTRACT (Continue on reverse if necessary and identify by block number)

Computer generated Fourier transform matched filters have been constructed using e-beam lithography. These filters were then evaluated by placing them in a VanderLugt optical correlator and addressing them with the original scene used to make the filters. Results show that the spatial frequency content of a filter may be tailored so as to obtain good signal-to-noise correlations while maintaining high diffraction efficiency.

20 DISTRIBUTION/AVAILABILITY OF ABSTRACT ☐ UNCLASSIFIED/UNLIMITED ☒ SAME AS RPT. ☐ DTIC USERS	21 ABSTRACT SECURITY CLASSIFICATION UNCLASSIFIED
22a. NAME OF RESPONSIBLE INDIVIDUAL Don A. Gregory	22b TELEPHONE (Include Area Code) (205) 876-7687 22c. OFFICE SYMBOL AMSMI-RD-RE

DD FORM 1473, 84 MAR 83 APR edition may be used until exhausted.
All other editions are obsolete.

TABLE OF CONTENTS

LIST OF ILLUSTRATIONS

LIST OF ILLUSTRATIONS (Continued)

I. INTRODUCTION

Digital techniques have much to offer in optical processing, although full digital integration into optical systems awaits development of spatial light modulators (SLM's) with high space-bandwidth and time-bandwidth products. The development of digital optical techniques can proceed, however, with such elements as digitally designed filters-constructed by e-beam or laser lithographic facilities. Facilities with this technology have proliferated in support of the electronic circuit industry.

Matched filters for use in optical correlators were previously constructed on the optical bench and in the photo lab. It is now possible to digitally design filters which give high signal-to-noise ratios when compared to analog produced filters. This is achievable because the filters may be "tailored" to accomplish special types of operations, such as high pass filtering. Additionally, during the design of these filters, simulations of their optical correlator response may be accomplished before actually having the filter fabricated. This saves time and fabrication expense.

The ability to design and fabricate digital matched filters opens several areas of development, If this technology is to be optimally utilized, several questions need to be answered:

(1) What is the best method of encoding complex numbers, representing an optical field, onto an optical plate or SLM?

(2) Beyond the encoding technique, what advanced filters can be developed to accomplish special tasks, such as obtaining multiplexed responses from a single filter?

(3) What are the best architectures for accomplishing optical processing (including matched filtering) based on digitally addressed SLM's?

II. THEORY

There are many ideas of how to encode two-dimensional complex data onto plates, question (1), Section I. If the plates are to be binary transmission filters, one places apertures at various locations to represent amplitude and phase. Well known techniques by Brown and Lohman, Lee, Allebach, and others have been discussed in the literature [1,2]. The results presented here have successfully utilized one of the methods of Lee [3]. This method appears esoteric, being based on an obscure mathematical result, but it can be heuristically appreciated from a simple point of view.

In a coherent correlator, one wishes to encode a representation of the Fourier transform of the object $h(x,y)$, which we call $H(u,v)$. This is a set of complex numbers, and we consider encoding the real quantity:

$$F = 1/2(H + H^*) = A \cos \phi,$$

where A and ϕ are the amplitude and phase of the Fourier transform, and are functions of the position points (u,v) in the Fourier plane.

The effect of encoding both H and H^* is that the transforms of the desired object and its inverse are both encoded - perhaps a desirable result. The Lee method, used in the results to be presented, requires the evaluation of F on a rectangular grid of contiguous rectangular cells. If the cosine phase term is positive within a cell, an aperture of fixed width (the cell width) is opened, with height proportional to the amplitude A. It is not apparent that this should give a meaningful encoding. Consider, however, adding a constant offset B, to F, so that it is everwhere positive. An aperture is then opened at each cell, with a constant width, but having a height proportional to $A \cos \phi + B$. The validity of this, as an encoding of the matched filter, can be established using the sampling theorem. Current simulation results, not presented here, show this technique to be somewhat superior to the Lee method. It is now heuristically clear that the transform is encoded as well as its conjugate, plus a constant bias. The effect of the offset bias is the creation of a bright spot on axis in the correlation plane, which in actual application becomes an image of an input to the correlator. The effect may prove to be undesirable.

Further work on encoding methods should be considered. The type of encoding may affect the variety of special filters which are possible. For example, the space-bandwidth product available on the fabricated filter is critical for many encoding techniques. Presently, using e-beam lithography, one may write minimum size apertures of about 0.5 micrometer (μm) incremented by 0.1 μm. This limits the dynamic range available (a critical factor), and the usable optical space-bandwidth product. Current results show that, even with such limits, quite useful filters can be obtained for a single object. The requirements based on these factors for multiplexed filters must still be evaluated - most likely by simulation. Optical reduction of fabricated filters may also be an important technique for laboratory study of this question. Such research defines the requirements for spatial light modulators needed to accomplish advanced filtering applications.

There are many applications of digital filters in optical systems that must be considered in discussion of question (2), Section I. If one has an input f(x,y) and desires an output g(x,y), then a filter representation of the function, (in the Fourier domain):

$$M(u,v) = G(u,v)/F(u,v)$$

is needed. A matched filter is obtained with G taken to be a constant - or inputs from a set of functions $\{f_i\}$, and outputs to a set $\{g_j\}$ may be desired. This is the multiplexing problem. Such special advanced digital filters may be studied through simulation; which must include various encoding techniques. These studies are different from normal digital simulations as they must also evaluate encoding algorithms, and may indicate new encoding techniques.

The VanderLugt correlator architecture awaits an SLM which can be digitally addressed to accomplish its full potential in the field, question (3), Section I. Correlation and convolution may be accomplished in the input plane (incoherently) at TV frame rates using other architectures, with SLMs which can be digitally addressed. The study of the optimum use of each type of architecture must give consideration to questions involving the potential for developing advanced filters, and to the available (or projected) performance parameters of SLMs.

Results are presented in this report for three filters - digitally designed and simulated by Applied Research using a Digital Hologram Development System configured from a Titan vision system with four megabytes of added memory. These filters were computed with x-y resolution of 1024 by 256 pixels, and encoded with methods similar to that described above. This resolution provides maximum sampling along the x axis and allows a large amount of variation of the aperture height (dynamic range) in the y direction. Aperture size was 4 μm wide by a maximum height of 16 μm.

The first filter produced in this series consisted of the Fourier transform of a tank image shown in Figure 1, encoded by the Lee method - except multiplied by the Fourier representation of a del-squared Guassian function, which takes on its maximum value at the edge of the filter. This is a form of high-pass filtering. A simulated signal to background of about 3000 was found for this filter correlated with a clean input scene. A photograph of this filter is given in Figure 2. The second filter produced was a binary phase only (BPO) construction made from the same tank Fourier transform and encoded by the Lee method. Phase only information was obtained by encoding all amplitudes as maximum. This filter gave a simulated signal to background of 632 correlated with a clean input scene. A photograph of this filter is given in Figure 3. The third filter produced was made from the same tank except that no actual amplitude information was used in the encoding. The Lee method was again used, but the apertures were artifically increased from zero in the center to a maximum on the edge, following a quadratic increase. This is similar to, but not the same as, the first filter. A simulated signal to background of 9000 was found in correlation with a clean input scene. A photograph of this filter is given in Figure 4.

Figure 1. Input scene used to construct the computer generated matched filters. The same scene was used to address the fabricated filters.

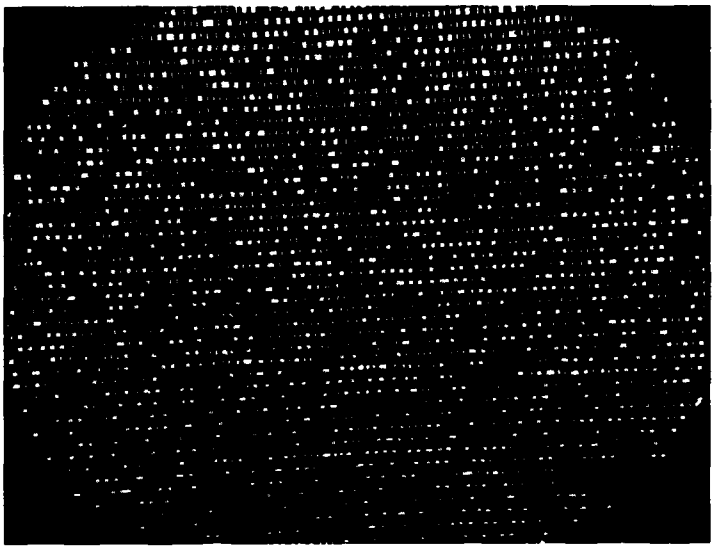

Figure 2. A photograph of the del-squared Gaussian profile filter. The magnification is about 100. The exposure time was 1/60 second.

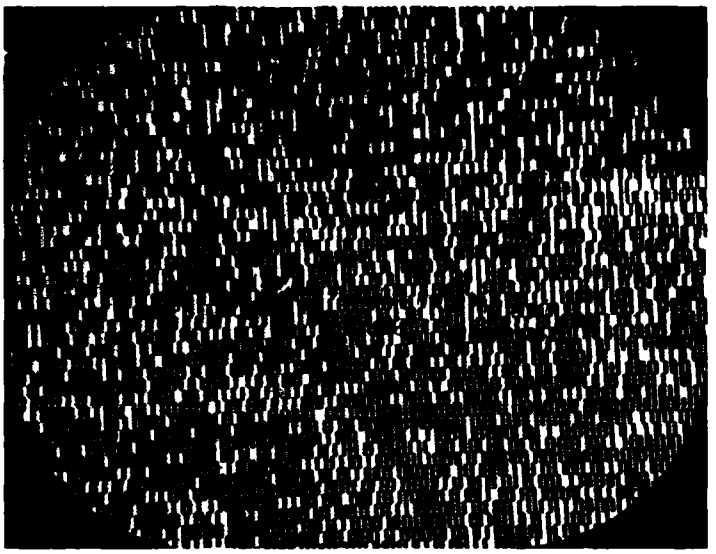

Figure 3. A photograph of the BPO filter. Magnification is about 100. The exposure time was 1/60 second.

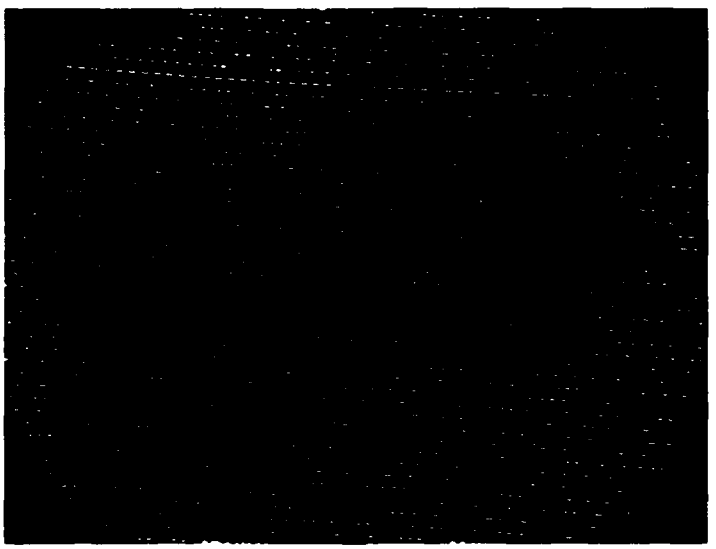

Figure 4. A photograph of the quadratically tapered filter (X^2). Magnification is about 100. Apertures were increased from zero in the center to a maximum at the edge of the filter. The exposure time was 1/15 second.

These filters worked very well, but they represent only the most elementary tests in applying digital techniques to optical filter construction. They were encoded with only a single object (although upright and upside down), using only straightforward encoding methods. Multiplexed, aspect and scale invariant filters, and filters optimized against a noise background have yet to be demonstrated.

III. EXPERIMENTAL PROCEDURE AND RESULTS

The experimental test of the computer generated matched filters (CGMF), was accomplished using the familiar VanderLugt arrangement shown in Figure 5, [4]. The filters were placed in the system at the focal plane of lens 2. The coherent input scene was provided by a Hughes Liquid Crystal Light Valve (LCLV). The photograph used originally to generate the CGMF was used also to address the filters. These filters had many characteristics common to their emulsion type counterpart having no rotational, scale or aspect invariance encoded. Therefore, a technique had to be developed so that these variables could be very closely matched to those used for the generation of the CGMF. A technique which proved to be successful involved placing a beamsplitter between the Fourier transform lens (L_2), and the CGMF. This allowed the addition of a separate HeNe laser beam which impinged upon the filter normally. This is shown in Figure 6. The thin second beam allowed the optical reconstruction of the originally encoded image. This reconstruction occurred off-axis so that the addressing image, on-axis from the LCLV, could be viewed simultaneously. The input scene was then rotated and scaled (using a zoom lens) until the two images matched. A photograph taken of the images is given in Figures 7, 8, and 9. The aspect angle was not a problem because the addressing image was a photograph, not a three-dimentional object. The final critical alignment involved moving the CGMF so that the Fourier transformed image addressed the filter correctly. This is always a difficult task, even when using a photographically stored filter. A misalignment of only a few μm is usually sufficient to cause a loss of the correlation signal [5]. This difficulty was compounded when the phase-only filters were addressed. There was no dark exposed central spot to align to. A tedious step and search was required before the correlation signal was observed. When the correct alignment was achieved however, the correlation beam was easily observed. The photograph of Figure 10 was taken by exposing a Polaroid type 55 film placed about 25 centimeters (cm) behind the CGMF. The filter addressed in this case was the BPO CGMF. The undiffracted portion of the addressing image was visible along with the correlation signals. The source of the multiple images and multiple correlations lies within the algorithm used to generate the CGMF.

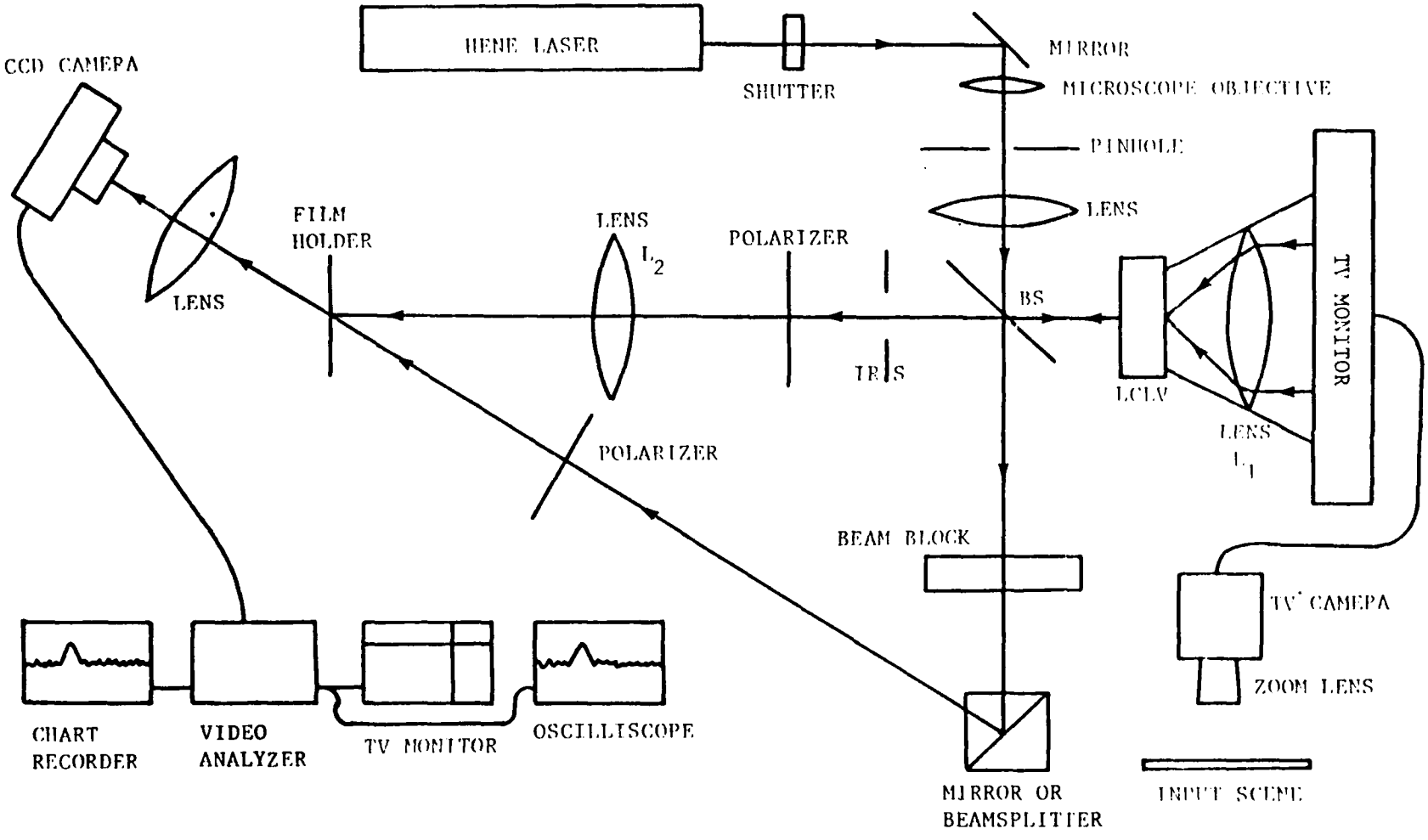

Figure 5. The real time optical correlator experimental arrangement.

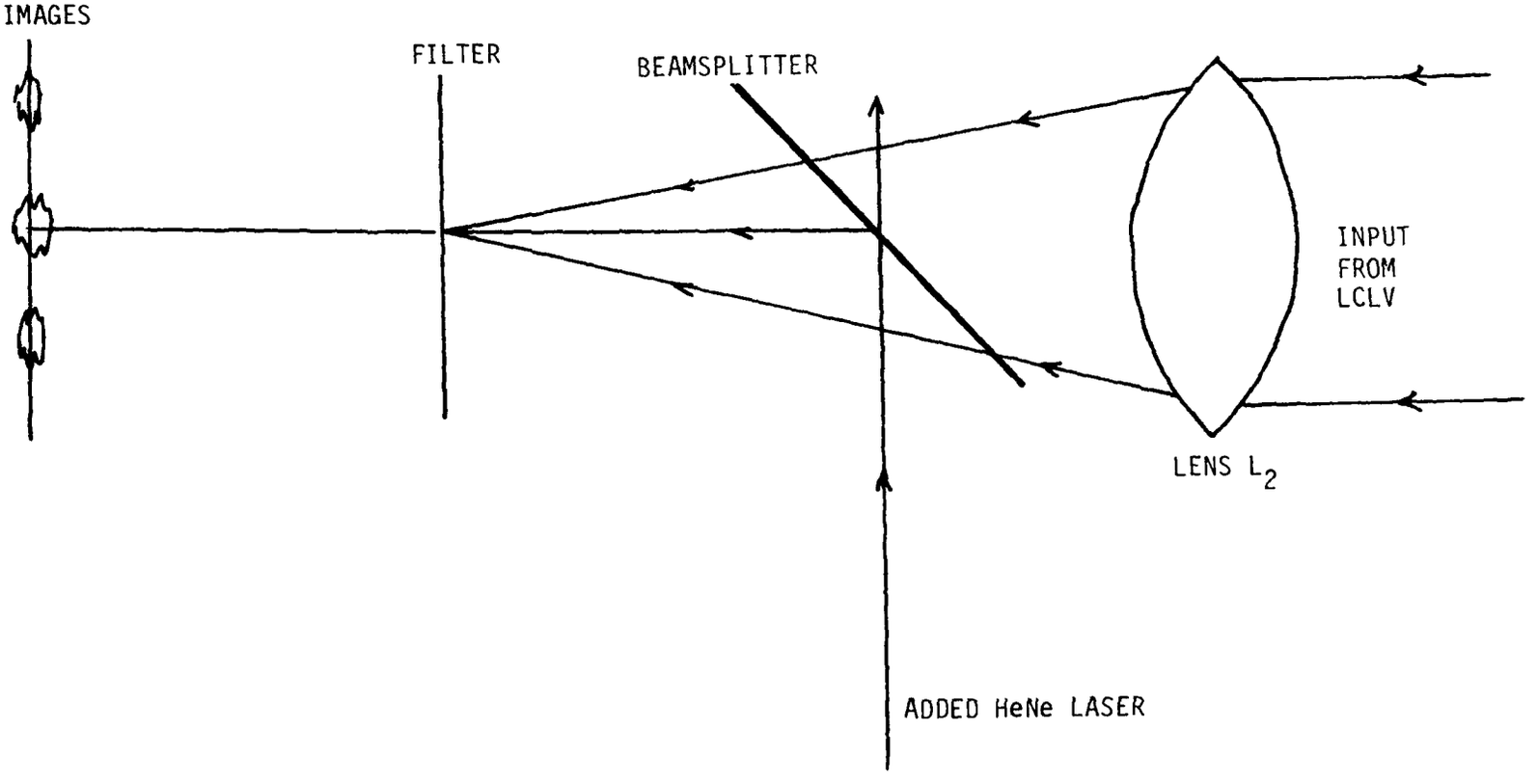

Figure 6. Technique used to observe the reconstruction from the filter and the addressing image simultaneously.

Figure 7. Simultaneous display of the addressing image (center) and the reconstruction from the BPO filter.

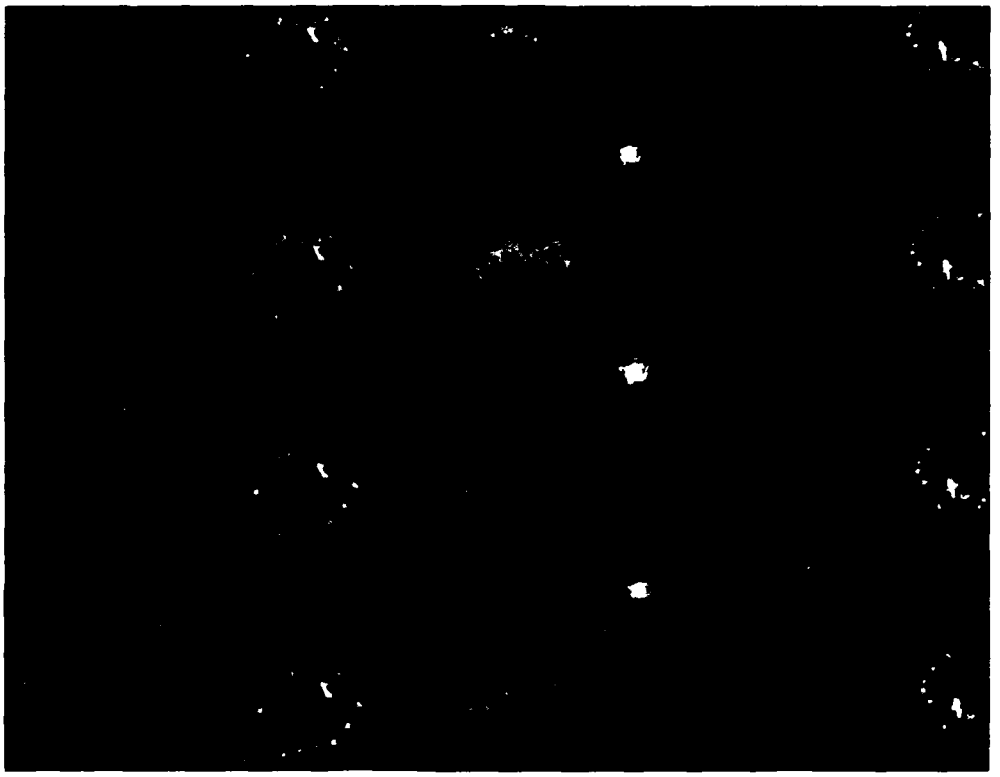

Figure 8. Simultaneous display of the addressing tank image (center) and the reconstruction from the quadratically tapered filter.

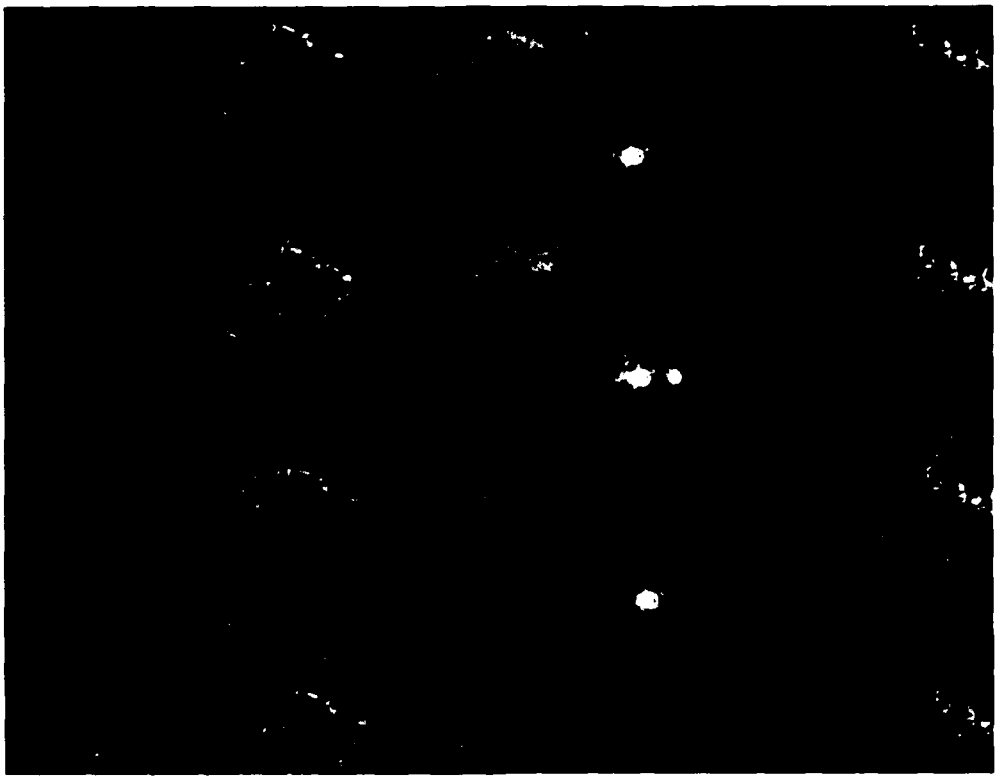

Figure 9. Simultaneous display of the addressing tank image (center) and the reconstruction from the del-squared Gaussian filter.

Figure 10. A photograph of the addressing tank image and the correlation signals resulting from the BPO filter. The exposure time was about 0.2 seconds.

The BPO filter exhibited a high diffraction efficiency. The correlation signal was quite pronounced and easily visible to the eye. The correlation signals from conventional matched filters are usually not visible to the eye. This is a result of the Kodak 649F film that is often used to record the filters. The diffraction efficiency is typically less than 0.5 percent. The diffraction efficiency of the BPO filter was about 2 percent. This represents a substantial increase.

A noisy background can be seen in Figure 10. This is somewhat typical for phase-only filters [6]. An intensity profile of the correlation signal and background is given in Figures 11 and 12. The sensitivity of the correlation signal to scale and rotation of the scene is a useful measurement and depends strongly on the spatial frequency content of the scene and filter. In general, a high spatial frequency content implies a strong sensitivity to these parameters. Results of measurements of this sensitivity are given in Figures 13 and 14. The data of Figures 11, 12, and 13 were taken using a Colorado Video image digitizer shown in the system drawing of Figure 5. A photograph of the correlation signal detected by the television camera and displayed on a TV monitor is given in Figure 15.

The X^2 contour filter was the next to be addressed using the optical correlator. Figure 16 gives the results which look similar to those obtained for the BPO filter. It is important to note that the exposure time of Figure 16 is about a factor of 10 longer than that of Figure 10. The diffraction efficiency measured was about 1 percent. The intensity profile of the correlation spot is given in Figures 17 and 18. The distribution is not very different from the BOP filter profile. Scale and rotational sensitivity is given by the curves in Figures 19 and 20. This filter is slightly less sensitive to rotation than the BPO, but comparable in sensitivity to scale. A photograph of the correlation spot as displayed on a video monitor is given in Figure 21.

The final filter to be evaluated was the del-squared Gaussian profile. The correlation spot and input image are shown in Figure 22. The exposure time was also about a factor of 10 longer than that used in Figure 10. The diffraction efficiency into the negative first order correlation spot was about 1 percent. The intensity profile of the correlation spot is given in Figures 23 and 24. The correlation spot was not circular; neither were the previous signals. This profile is not very different from the previous two. Figures 25 and 26 give the scale and rotational sensitivities. This filter is the least sensitive of the three to scale and rotation. A photograph of the correlation spot displayed on a video monitor is given in Figure 27. All three filters produced correlation spots well above background noise and easily observed with the eye. It was necessary to include a pair of polarizers in front of the CCD television camera used to detect the signals, so as to avoid saturation.

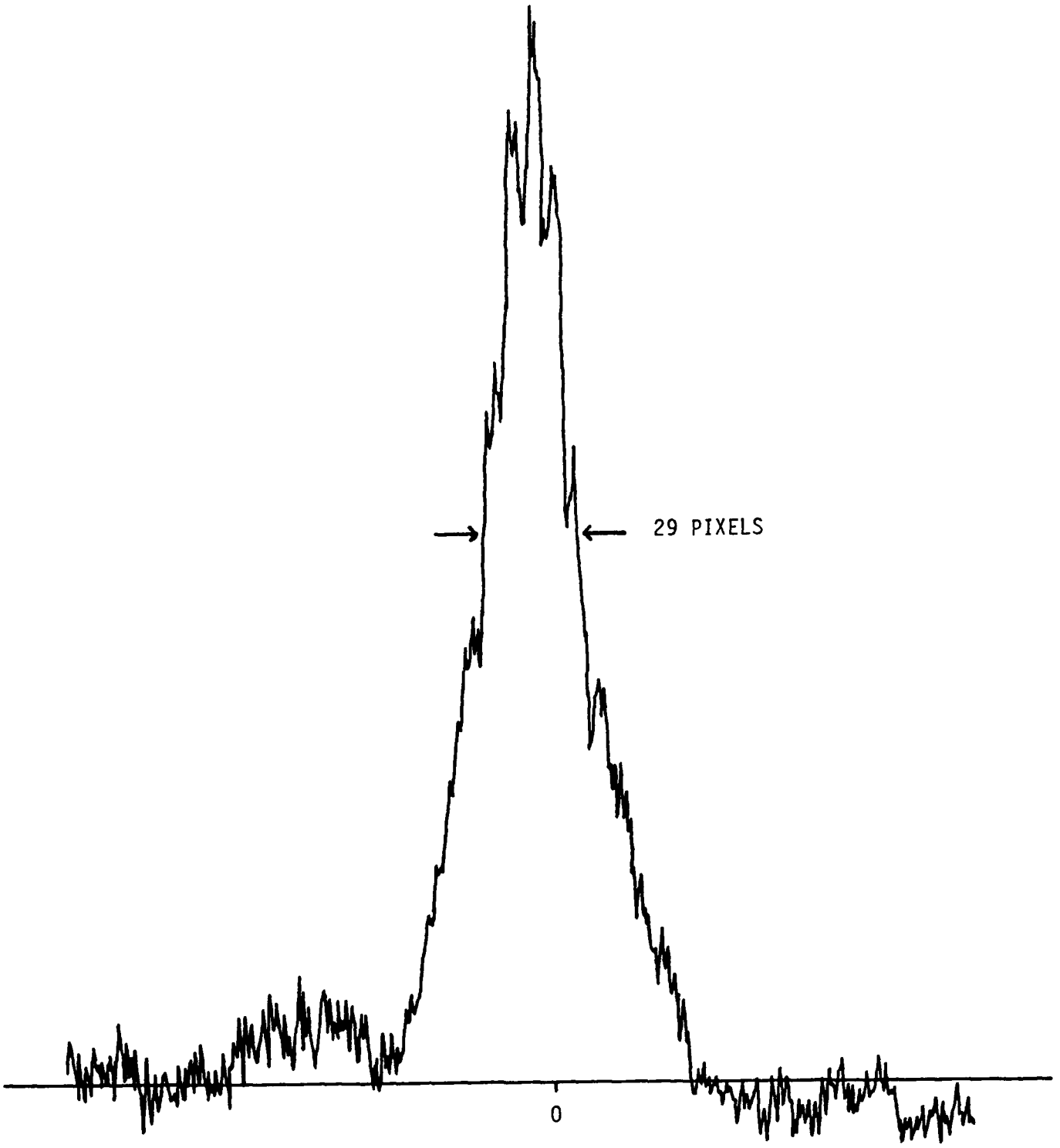

Figure 11. Horizontal sweep through the correlation spot as displayed on a television monitor and digitized by the Colorado video image digitizer. This data is for the BPO filter.

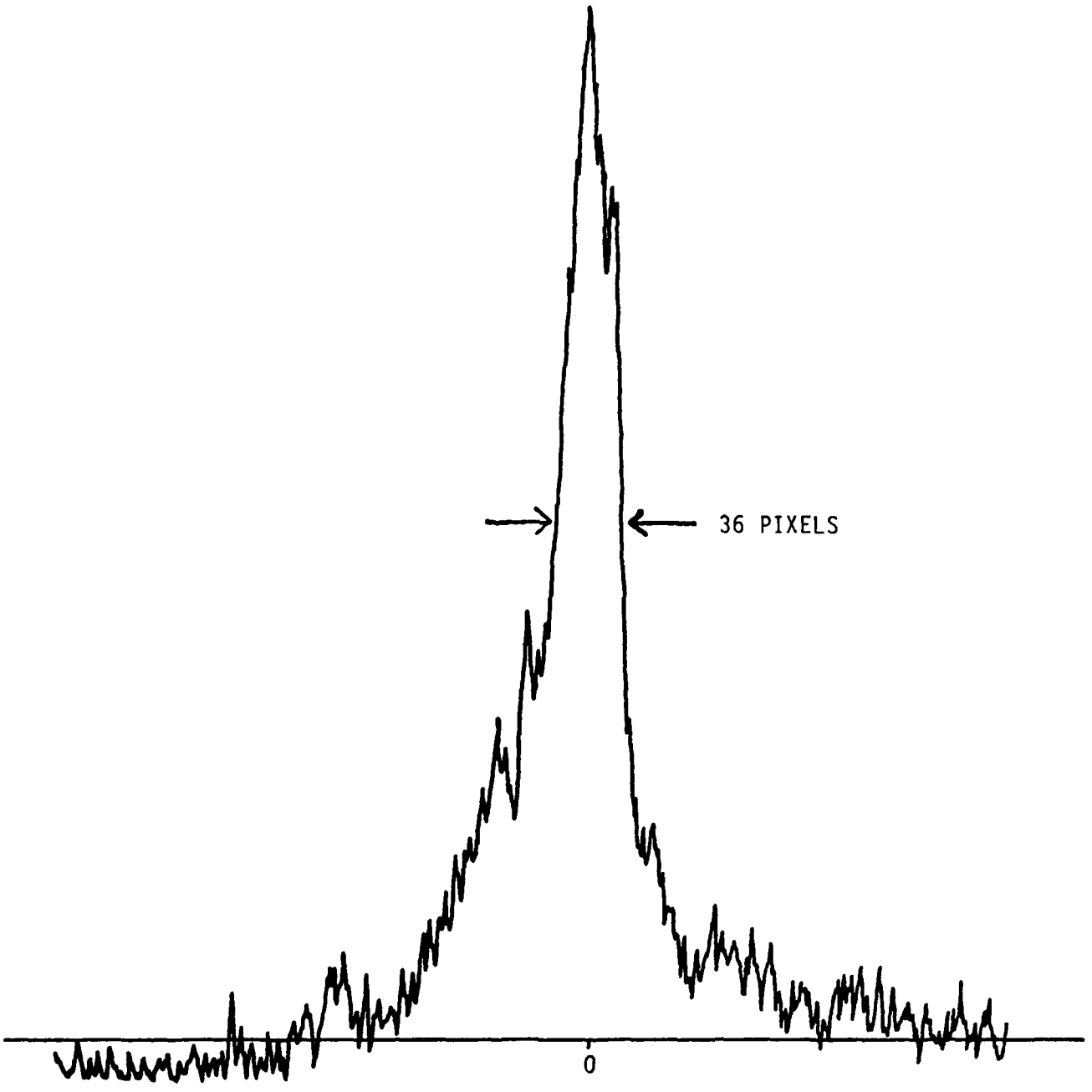

Figure 12. Vertical sweep through the correlation spot produced by the BPO filter.

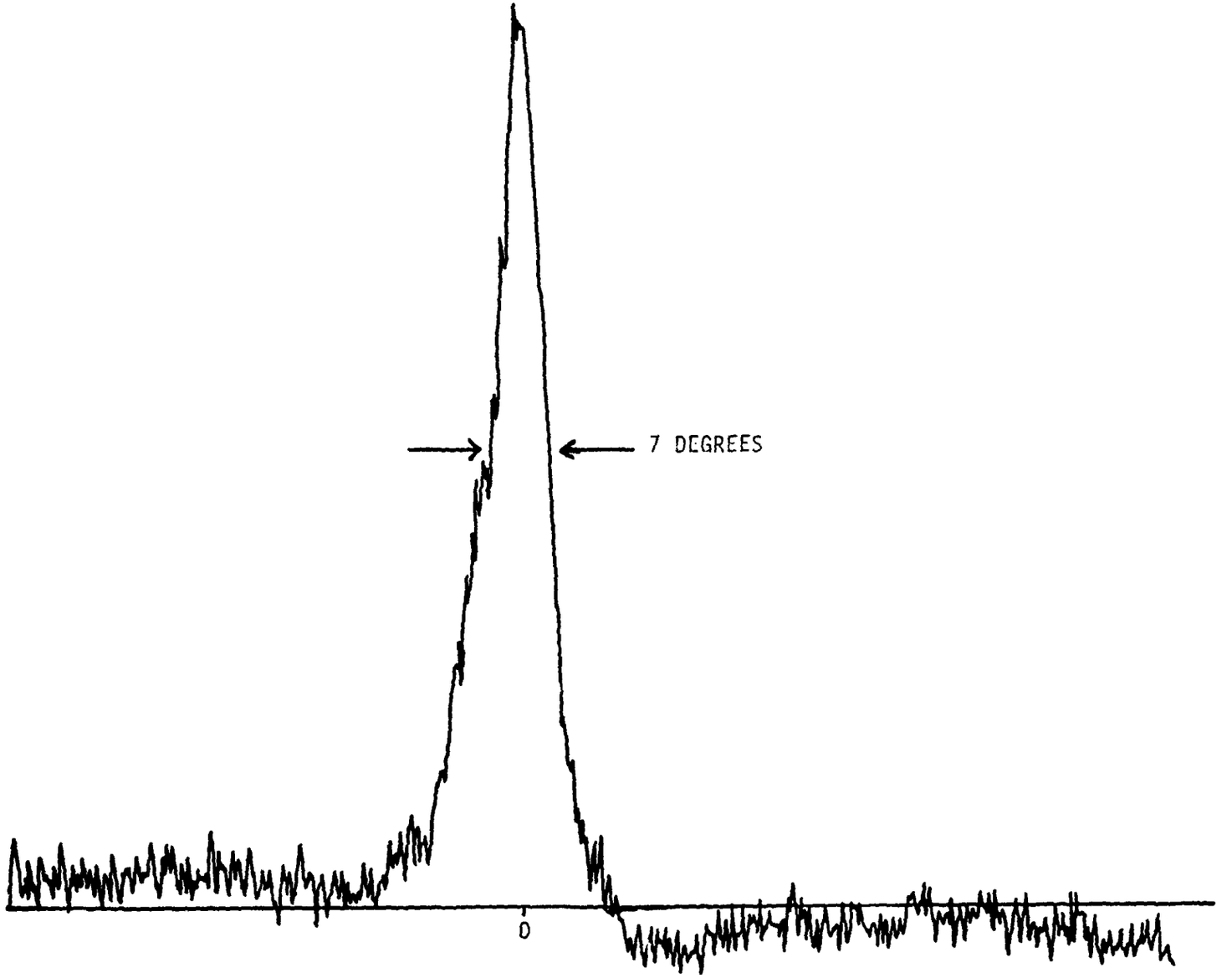

Figure 13. Rotational sensitivity of the BPO filter.

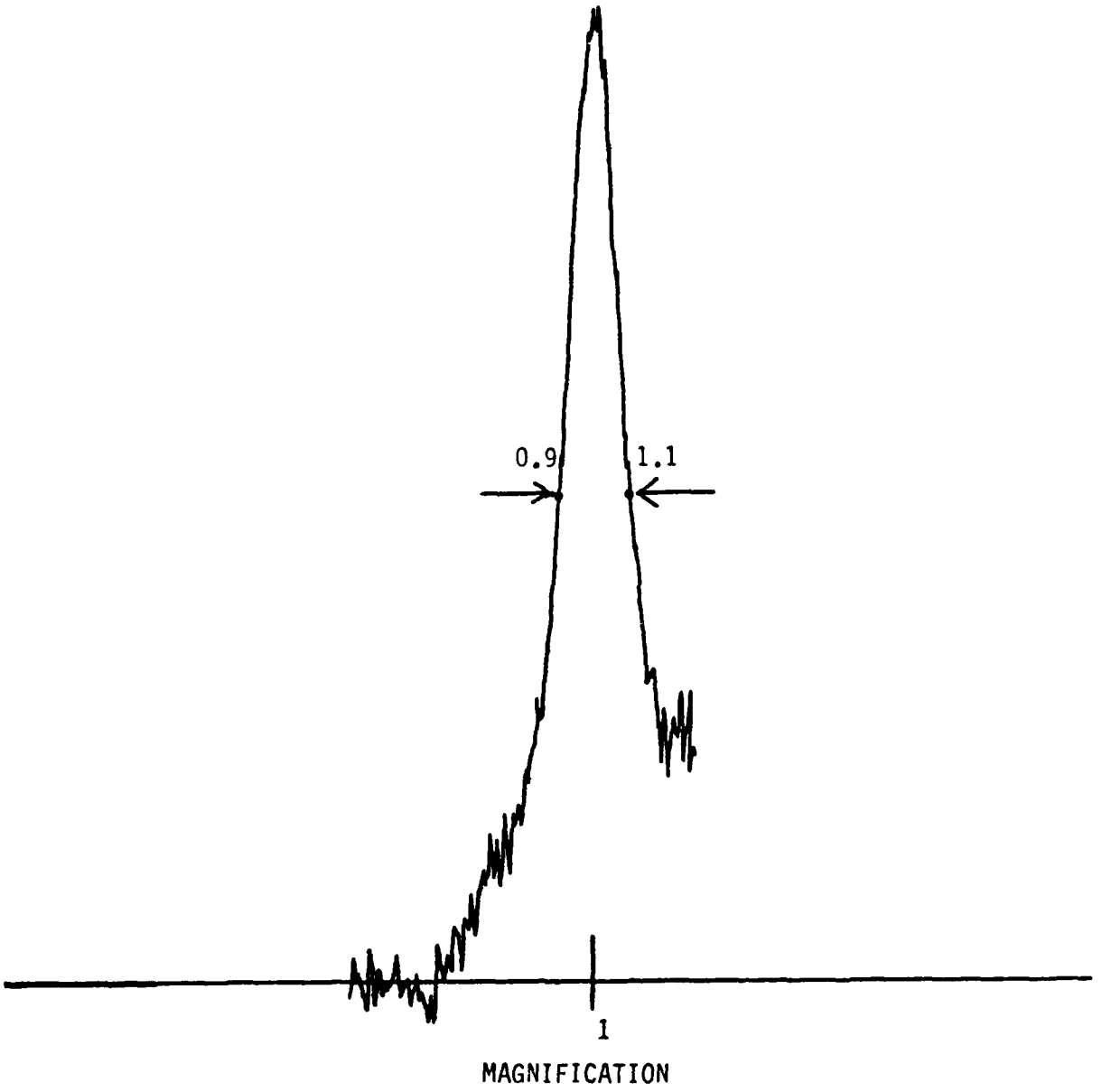

Figure 14. Scale sensitivity of the BPO filter. It was not possible to increase the size of the image more than about 20 percent.

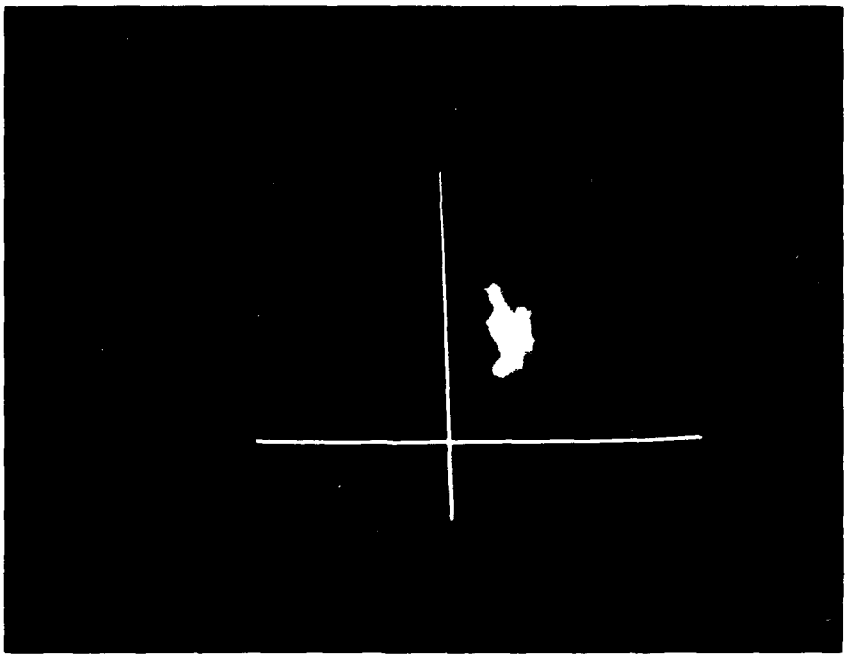

Figure 15. A photograph of the television screen displaying the correlation spot produced by the BPO filter. The axes of the Colorado video image digitizer are also visible. Exposure was 1 second.

Figure 16. A photograph of the addressing tank image and the correlation signals resulting from the quadratically tapered filter. The exposure time was about 3 seconds.

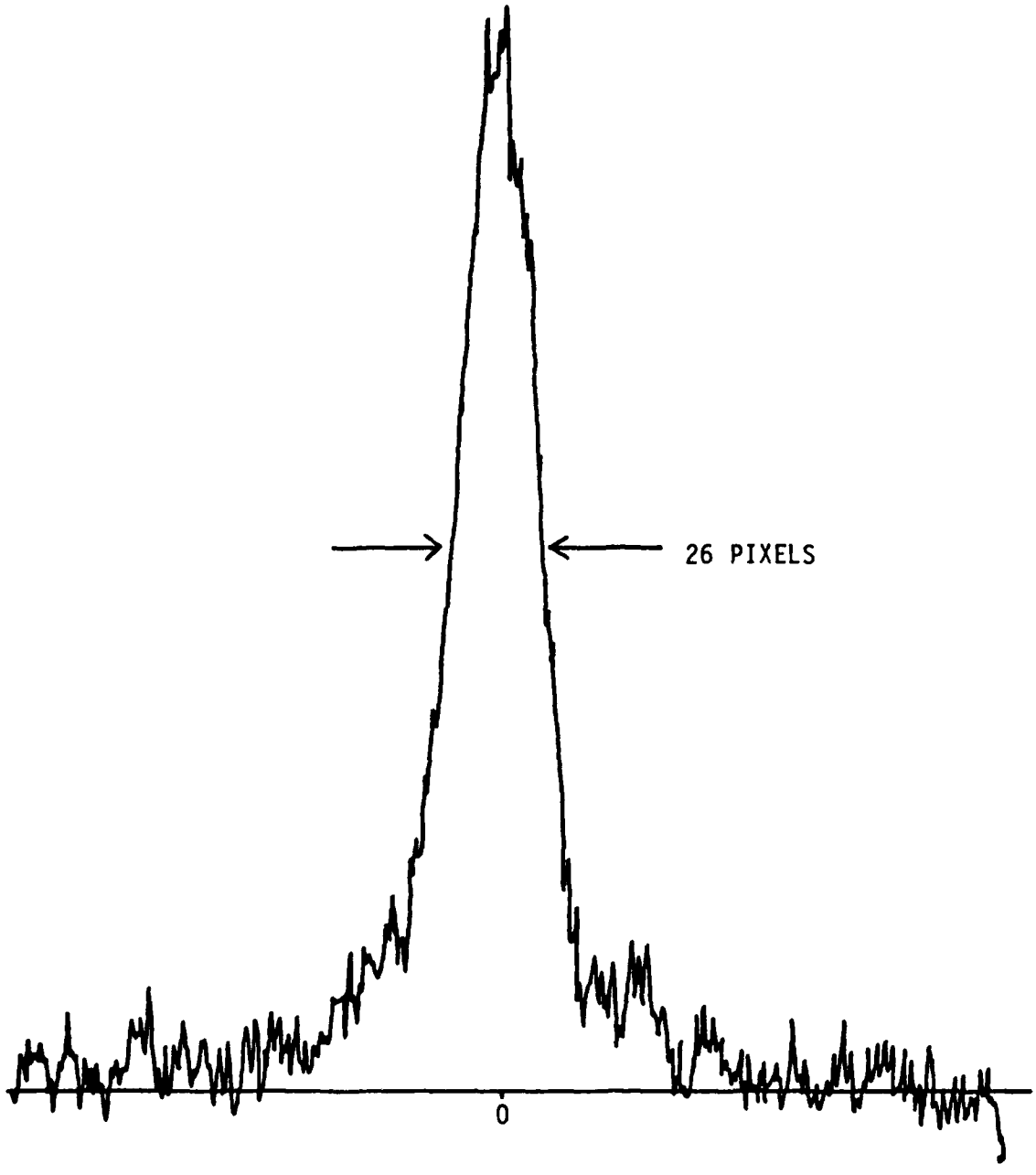

Figure 17. Horizontal sweep through the correlation spot from the phase-only Gaussian filter.

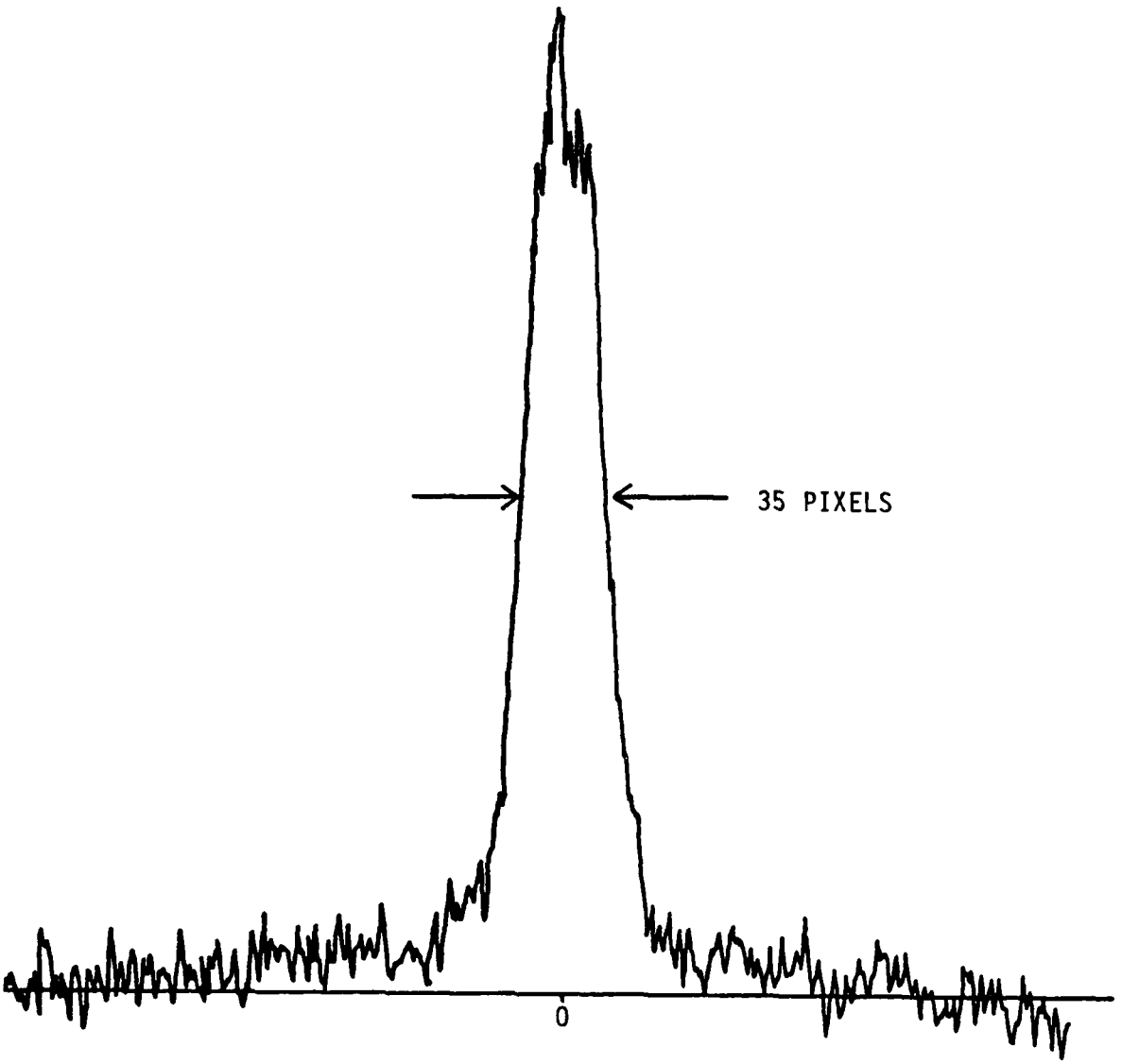

Figure 18. Vertical sweep through the correlation spot produced by the phase-only Gaussian filter.

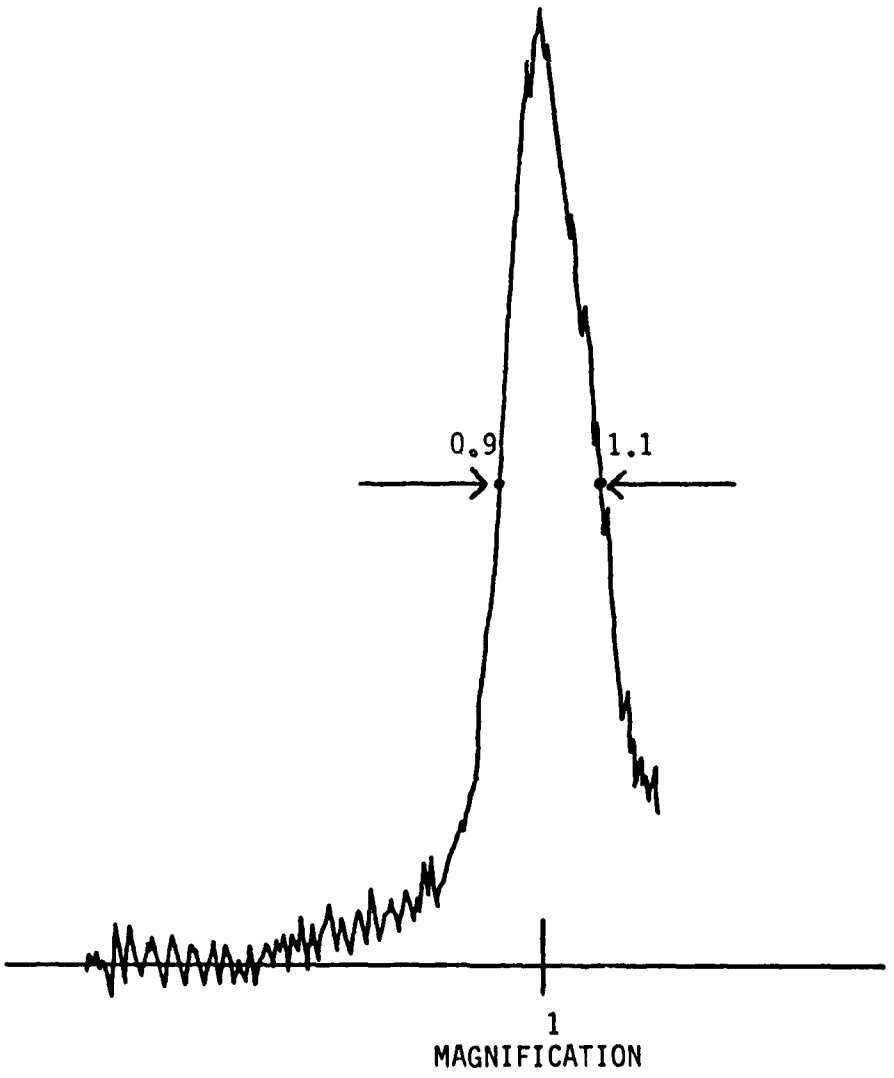

Figure 19. Scale sensitivity of the phase-only Gaussian filter. Equipment limitations prevented a magnification greater than about 1.2.

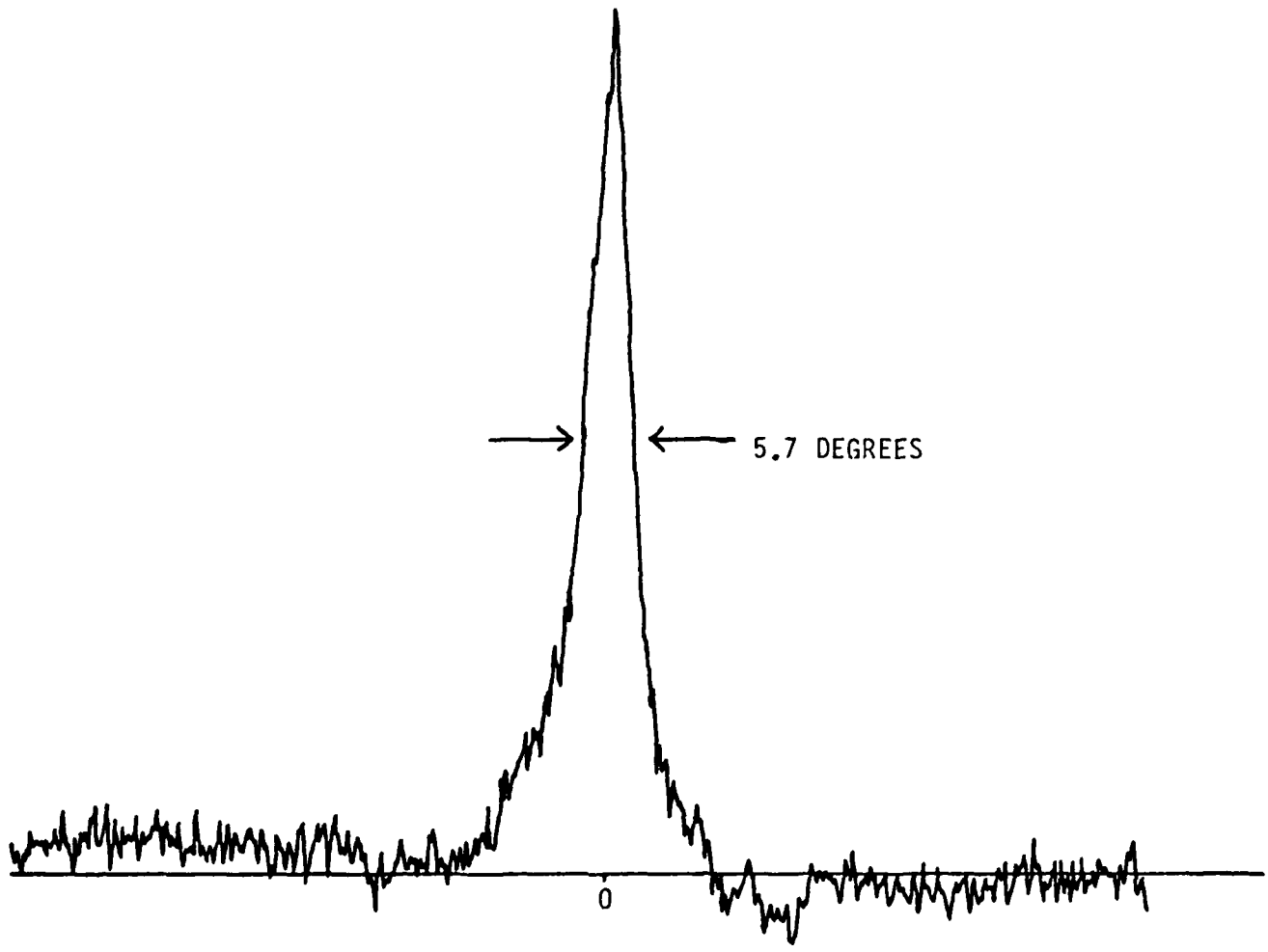

Figure 20. Rotational sensitivity of the phase-only Gaussian filter.

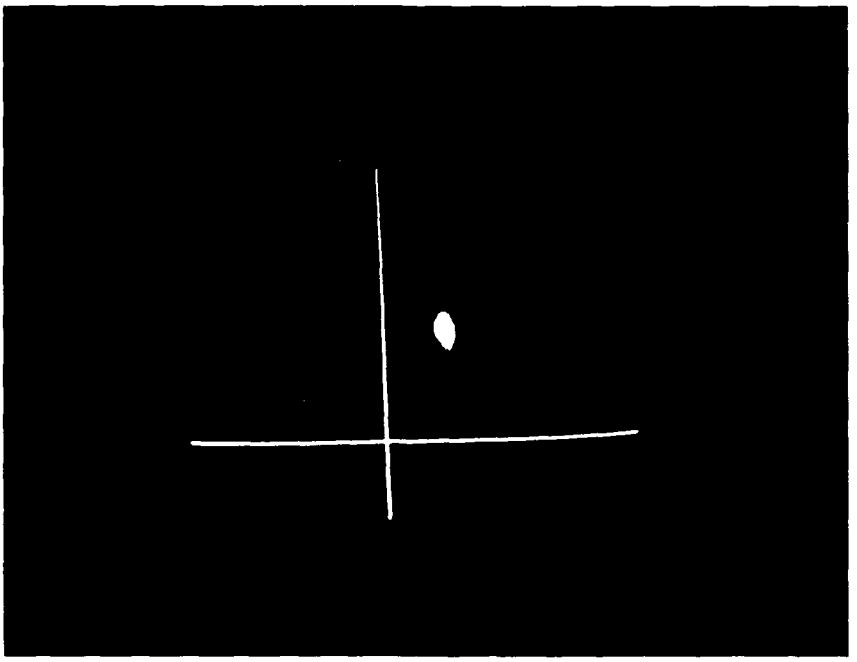

Figure 21. Correlation signal as displayed on a television monitor for the quadratically tapered filter. Exposure time was 1 second.

Figure 22. A photograph of the addressing tank image and the correlation signals resulting from the del-squared Gaussian filter. Exposure time was about 3 seconds.

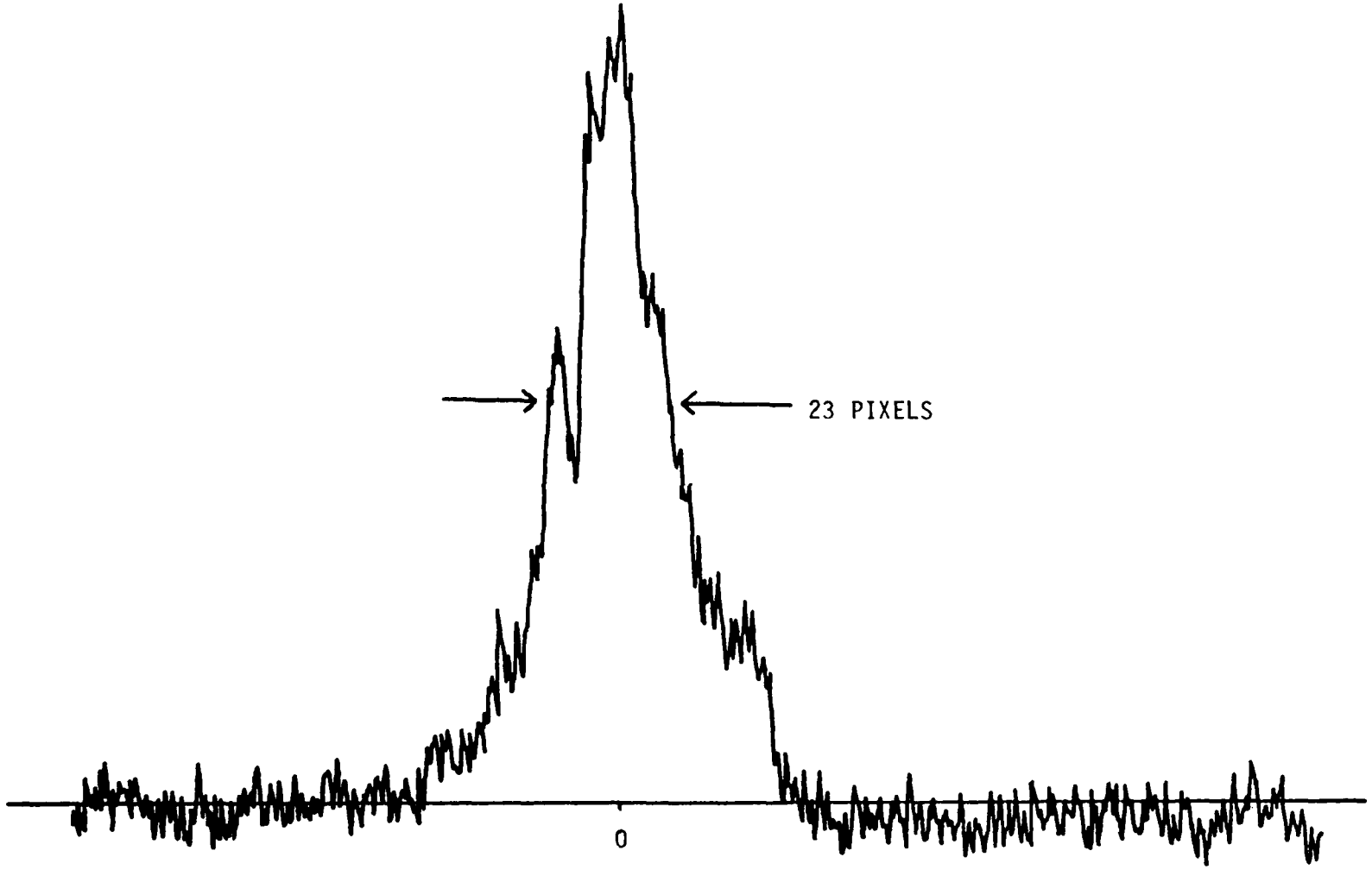

Figure 23. Horizontal sweep through the correlation spot resulting from the amplitude Gaussian filter.

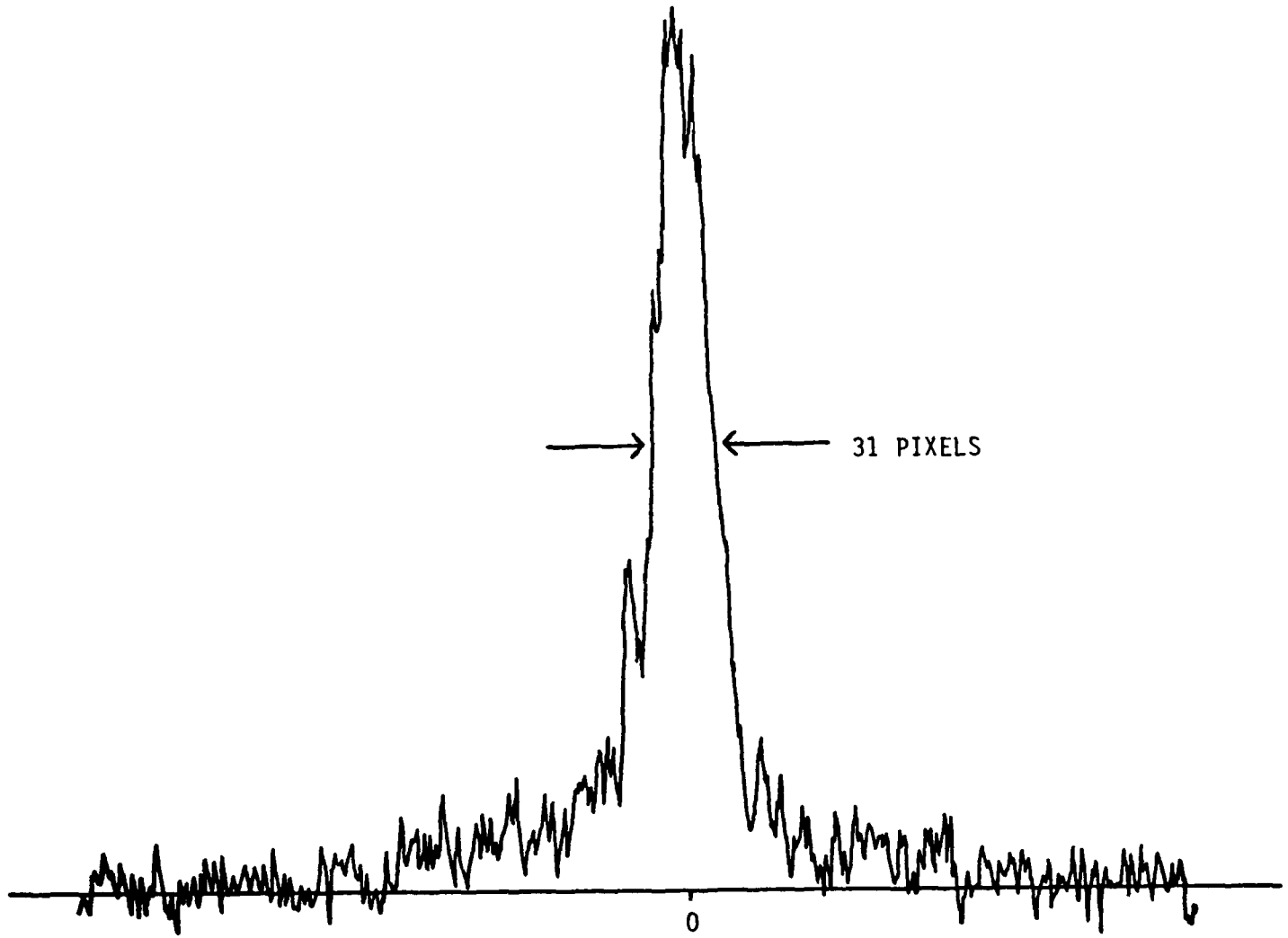

Figure 24. Vertical sweep through the correlation spot resulting from the amplitude Gaussian filter.

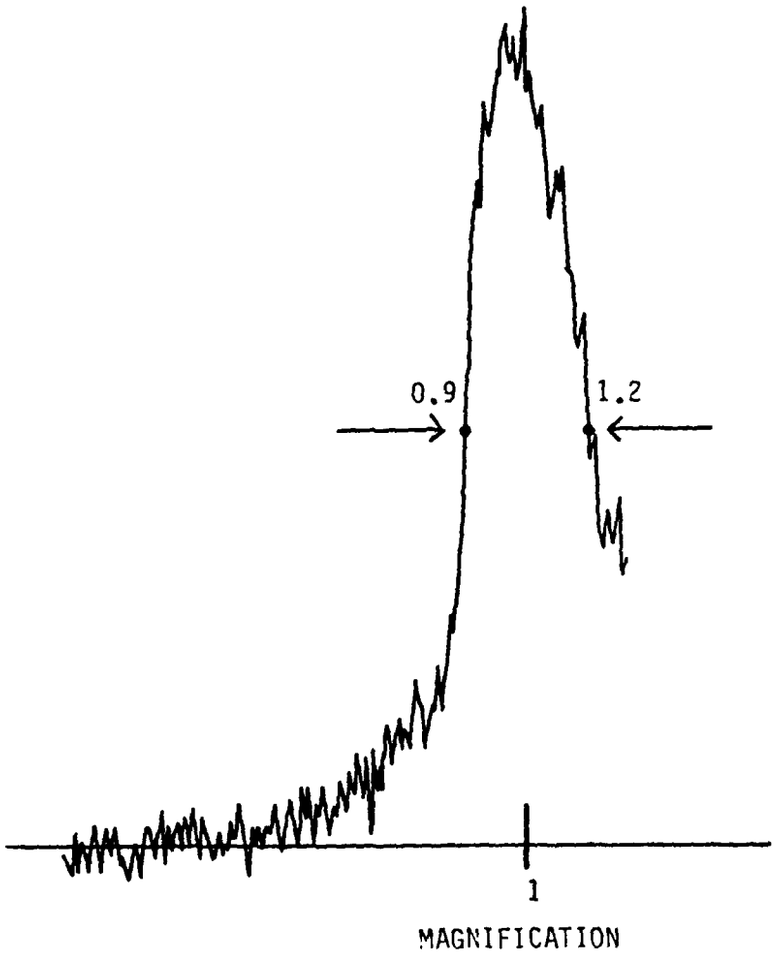

Figure 25. Scale sensitivity of the amplitude Gaussian filter.

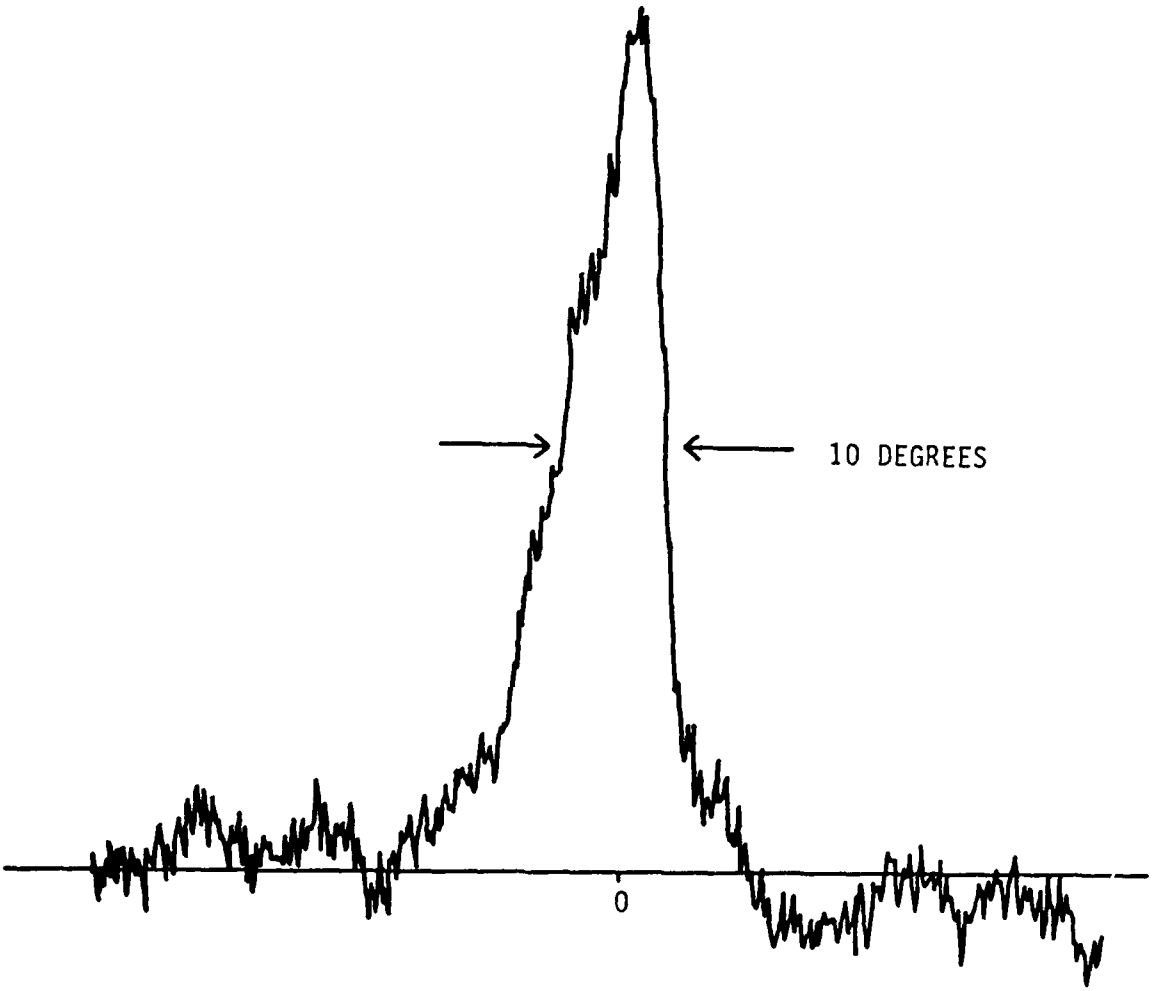

Figure 26. Rotational sensitivity of the amplitude Guassian filter.

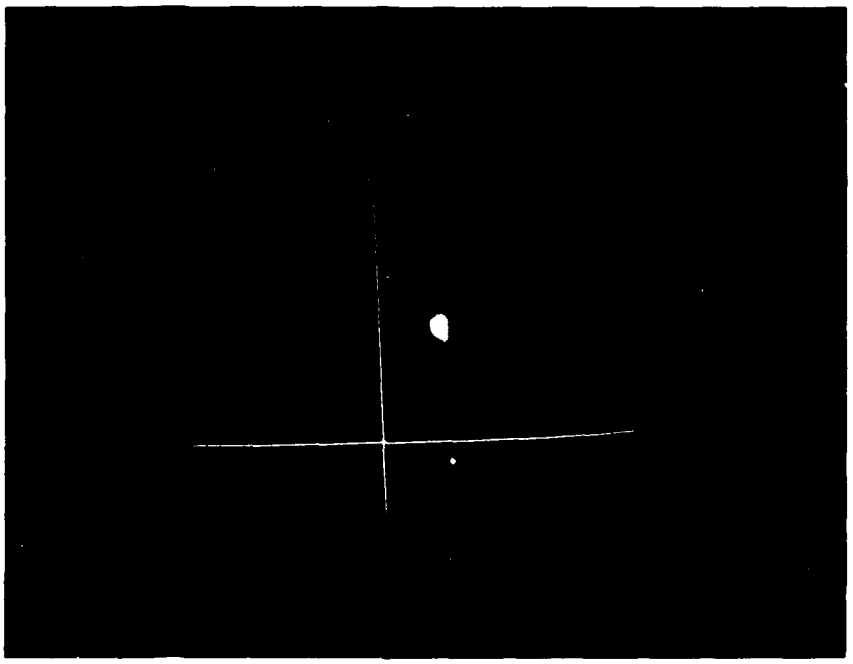

Figure 27. Photograph of correlation spot as displayed on a television monitor for the amplitude Gaussian filter. Exposure time was about 1 second. The crosshairs from the Colorado video image digitizer are also visible.

IV. DISCUSSION

The results presented in this report are the first attempts toward modifying the spatial frequency content of computer generated matched spatial filters. Conventional holographic matched filters suffer from having a large portion of the incident energy of the image being contained in the lower spatial frequencies. This generally causes an overexposure of the lower frequencies and an underexposure of the higher frequencies while making the matched filter. Computer generated matched filters offer the capability of manipulating the spatial frequency content.

All three filters exhibited a high diffraction efficiency when compared to their holographic emulsion counterpart. The BPO filter was highest in diffraction efficiency, but also the highest in background noise. The long exposure photograph of Figure 28 shows the noisy background. The physical size of the correlation spot is governed by the spatial frequency content of the filter and scene. In general, high spatial frequency filter/scene combinations produce small correlation spots (5-10-pixels in diameter) while low spatial frequency filters/scenes produce much larger spots. The latter case has been observed in the three filters investigated in this report. Much smaller correlation spots have been obtained using the identical experimental arrangement and Silver Halide holographic film (Kodak 649F) as the recording medium. Therefore, it is reasonable to assume that the spatial frequency content of the computer generated filters investigated here is the governing factor in determining correlation spot size. Of course, the inverse should also be true. If high frequencies were encoded on the filter and only low frequencies were used to address the filter, the spot size should be large. The highest spatial frequency encoded on the filters was about 9 per millimeter. This is likely the chief cause of the large correlation spot. The liquid crystal light valve used in the experiment has a spatial frequency range at least a factor of three larger than that encoded on the filters. Higher frequencies should be encoded onto the CGMF if possible.

Other experiments performed included the measure of rotation and scale sensitivity of the correlation signal. These are typical measurements that have been made for emulsion type matched filters for several years using a wide variety of scenes. The results presented in this report can be compared to earlier findings. It is interesting to note that the most rotationally sensitive filter studied here was the quadratically tapered format. In general, it has been observed that the higher spatial frequencies produce the most rotationally sensitive filters. The quadratic filter emphasizes the higher frequencies while decreasing the role of the lower frequencies. However, this was also somewhat true of the del-squared filter which did not exhibit strong rotational sensitivity.

Figure 28. Long exposure photograph of correlation signal from BPO filter showing noisy background. Exposure time was 0.5 seconds.

The BPO filter, which had no spatial frequency tailoring, was more sensitive to rotation than the del-squared filter, but less sensitive than the quadratic. All three filters were less sensitive to rotation than their emulsion type counterparts. This is no doubt due to the lower spatial frequencies recorded on the CGMF's. A rotation of 1.5 to 2.5 degrees is usually sufficient to cause a 50-percent loss in correlation intensity for a typical Kodak 649F filter made using a scene similar to the tank photograph used in this investigation. The CGMF's addressed in this report could tolerate a scene rotation of about 3 to 5 degrees in either direction before losing 50 percent of the correlation intensity. The same general trend was true of scale changes. Normally a 2 to 5-percent change is enough to cause a 50-percent loss in correlation intensity. The CGMF's could tolerate a 10-percent scale change. A matched filter that is tolerant of rotation and scale changes is much desired but there is a price to pay. This is discussed in the next section.

V. CONCLUSION

This report represents the first attempts toward using spatial frequency tailored matched filters for recognition and tracking purposes. The experiment was successful in that matched filters were produced using e-beam lithography, and they demonstrated a high diffraction efficiency when addressed in a coherent real time VanderLugt type correlator. A definite tradeoff exists in deciding the spatial frequency bandwidth to be recorded. If high frequencies are emphasized (>50 mm^{-1}), then the correlation signal produced has a narrow width, which means that the location of the target scene may be known to a high degree of accuracy. Unfortunately, this also means that the correlation signal produced by the filter will be extremely sensitive to a rotation or scale change in the scene. This sensitivity can be lessened by emphasizing the lower spatial frequencies, but this produces a correlation spot that is broad in intensity, and not well localized. The latter case applies to the filters investigated in this report. The tapering of the spatial frequency content did not radically affect the correlation signals due to the spatial frequency bandwidth recorded onto the plates. The maximum spatial frequency (9 mm^{-1}) was quite low. Higher frequencies will have to be recorded before drastic differences will be observed.

The experiment was a success even though the tailoring effect was not as pronounced as expected. Three filters were calculated using different techniques, etched using e-beam lithography, and then successfully addressed using a VanderLugt coherent optical correlator. Better filters will be constructed in the future using the experience gained from this investigation.

REFERENCES

1. Brown, B. R., and Lohman, A. W., "Complex Spatial Filtering with Binary Masks," Appl. Opt., Vol. 5, p. 967, 1966.

2. Allenbach, J. P., "Representation Related Errors in Binary Digital Holograms: A Unified Analysis," Appl. Opt., Vol. 20, p. 290 1981.

3. Lee, W. H., "Binary Computer Generated Holograms," Appl. Opt., Vol. 18, p. 3661, 1979.

4. Guenther, B. D., Christenen, C. R., and Upatnieks, J. M., "Coherent Optical Processing: Another Approach," IEEE J. Quant. Elect., QE-15, No. 12, p. 1348, 1979.

5. Gregory, Don, and Huckabee, Laura, "Acoustooptically Addressed Fourier Transform Matched Filtering," Appl. Opt., Vol. 24, No. 6, p. 859, 1985.

6. Horner, Joseph, and Gianino, Peter, "Phased-Only Matched Filtering," Appl. Opt., Vol. 23, No. 6, p. 812, 1984.

DISTRIBUTION

	NUMBER OF COPIES
Director U.S. Army Research Office ATTN: SLCRO-PH ATTN: SLCRO-ZC P.O. Box 12211 Research Triangle Park, NC 27709-2211	1
Headquarters Department of the Army DAMA-ARR Washington, DC 20310-0632	1
Headquarters OUSDR&E The Pentagon ATTN: Dr. Ted Berlincourt Washington, DC 20310-9632	1
Defense Advanced Research Projects Agency Defense Sciences Office Electronics Systems Division ATTN: Dr. A. Yang 1400 Wilson Boulevard Arlington, VA 22209	1
Commander U.S. Army Foreign Science and Technology Center ATTN: AIAST-RA 220 Seventh Street, N.E. Charlottesville, VA 22901-5396	1
Director, URI University of Rochester College of Engineering and Applied Science The Institute of Optics Rochester, NY 14627	1
Director, JSOP University of Arizona Optical Science Center Tucson, AZ 85721	1
Electro-Optical Terminal Guidance Branch Armament Laboratory ATTN: Dr. Steve Butler Eglin Air Force Base, FL 32542	1

	NUMBER OF COPIES
U.S. Army U.S. Army Cold Regions Research and Engineering Laboratory ATTN: Dr. Richard Munis 72 Lyme Mill Road Hanover, NH 03755	1
Night Vision and Electro-Optics Center ATTN: AMSEL-NV-T, Mark Norton Building 357 Fort Belvoir, VA 22060	1
RADC/ESOP ATTN: Dr. Joseph Horner Hanscom AFB, MA 01731	1
Applied Science Division Applied Optics Operations ATTN: Mr. Jeff Sloan P.O. Box 3115 Garden Grove, CA 92641	1
Department of Electrical Engineering Stanford University ATTN: Dr. J. W. Goodman Stanford, CA 94305	
University of Alabama in Huntsville Center for Applied Optics ATTN: Dr. H. John Caulfield Huntsville, AL 35899	1
University of Alabama in Huntsville Physics Department ATTN: Dr. J. G. Duthie Huntsville, AL 35899	1
Carnegie-Mellon University Department of Electrical and Computer Engineering ATTN: Dr. David Cassasent Pittsburgh, PA 14213	1
Penn State University Department of Electrical Engineering ATTN: Dr. F. T. S. Yu University Park, PA 16802	1

	NUMBER OF COPIES
University of Alabama in Birmingham Physics Department ATTN: Mr. James F. Hawk University Station Birmingham, AL 35294	1
NASA Johnson Space Center ATTN: Code EE-6, Dr. Richard Juday Houston, TX 77058	1
Jet Propulsion Lab ATTN: Dr. Michael Shumate 4800 Oak Grove Drive Pasadena, CA 91109	1
Naval Weapons Center ATTN: Code 3941, David Bloom China Lake, CA 93555	1
University of Colorado at Boulder Department of Electrical and Computer Engineering ATTN: Dr. Kristina Johnson Boulder, CO 80309-0425	1
Naval Research Lab ATTN: Code 6537, Dr. Arthur Fisher Washington, D.C. 20375-5000	1
U.S. Army Materiel System Analysis Activity ATTN: AMXSY-MP Aberdeen Proving Grounds, MD 21005	1
IIT Research Institute ATTN: GACIAC 10 W. 35th Street Chicago, IL 60616	1
Perkin-Elmer Corporation ATTN: Dr. Robert Buzzard 2707 Artie Street, S.W. Suite 14 Huntsville, AL 35805	1

DISTRIBUTION (Continued)

	NUMBER OF COPIES
AMSMI-RD, Dr. McCorkle	1
Dr. Rhoades	1
Dr. Stephens	1
RD-RE, Dr. Bennett	1
RD-RE-OP, Dr. Charles Bowden	1
Dr. Don A. Gregory	80
Mr. David J. Lanteigne	1
Mr. James C. Kirsch	1
Mr. Tracy D. Hudson	15
RD-CS-R	1
RD-CS-T	1
AMSMI-GR-IP, Mr. Bush	1
DASD-H-V	1